

LASER INTERFEROMETER GRAVITATIONAL WAVE OBSERVATORY
- LIGO -
CALIFORNIA INSTITUTE OF TECHNOLOGY
MASSACHUSETTS INSTITUTE OF TECHNOLOGY

| |
|--|
| Document Type LIGO-T980101-00 - D 10/29/98 |
| Up-Conversion of Scattered Light Phase Noise from Large Amplitude Motions |
| Michael R. Smith |

Distribution of this draft:

xyz

This is an internal working note
of the LIGO Project.

California Institute of Technology
LIGO Project - MS 51-33
Pasadena CA 91125
Phone (626) 395-2129
Fax (626) 304-9834
E-mail: info@ligo.caltech.edu

Massachusetts Institute of Technology
LIGO Project - MS 20B-145
Cambridge, MA 01239
Phone (617) 253-4824
Fax (617) 253-7014
E-mail: info@ligo.mit.edu

WWW: <http://www.ligo.caltech.edu/>

LIGO DRAFT

1 INTRODUCTION

The phase noise introduced into the LIGO gravity wave signal, from light scattered by moving surfaces may have a frequency spectrum which exhibits harmonics of the fundamental motion frequency of the scattering surface. This effect will occur whenever the magnitude of the surface motion becomes comparable to the size of the wavelength of light. In fact the magnitude of the motion can even be considerably smaller than the wavelength, and harmonic distortion will still produce harmonics of the fundamental motion frequency. If the scattering surface motion becomes sufficiently large and exceeds 1/8 wavelength, the phase noise will “wrap fringes” and the resulting noise spectrum will contain a rich mixture of higher harmonics.

A quantitative analysis of harmonic phase noise generation will be given below. The results will be applied to determine the allowed limits on the resonant frequency and Q of the LIGO beam-dump structure.

2 PHASE NOISE SPECTRUM

Light of wavelength λ scattered out of the IFO and then re-scattered back into the IFO from a moving surface acquires a time varying phase shift $\Phi(t) = 4\pi\frac{x(t)}{\lambda}$, which adds phase noise to the gravity wave signal. The extra factor of 2 occurs because the light must travel twice the displacement distance of the scattering surface in order to complete the round trip back into the IFO. The noise contribution¹ added to the gravity wave signal is proportional to $\sin(\Phi(t))$.

2.1. Fringe Wrap

2.1.1. Scattering Surface Motion, Time Function

The noise contribution reaches its maximum value for $\Phi(t) = \frac{\pi}{2}$, which corresponds to $x_{max} = \frac{\lambda}{8}$. For larger values of x, the phase of the scattered light “wraps around to a new fringe”, so the apparent displacement is effectively clamped at $\frac{\lambda}{8}$. The clamped effective displacement of the scattering surface at the onset of fringe wrap has a time variation given by

$$x_{eqt}(t) = \frac{\lambda/8}{\max(\Phi(t))} \sin(\Phi(t)).$$

We will analyze the temporal response of the scattered light phase by assuming that the surface varies sinusoidally at a resonant frequency, f_0 .

$$\Phi(t) = A_s(f_0) \sin(2\pi f_0 t).$$

1. E. Flanagan and K. Thorne, “Noise Due to Backscatter Off Baffles, the Nearby Wall, and Objects at the Far end of the Beam Tube; and Recommended Actions”, LIGO-T940063

The amplitude of vibration will be taken to be the standard LIGO seismic ground noise spectrum¹ amplified by the response function of the resonant scattering surface.

$$A_s(f_0) := T(f_0) \cdot x_s(f_0)$$

And, the frequency response function of a scattering surface resonant at the frequency f_R with a damping coefficient of $1/Q$ is given by

$$T(f_0) := \frac{(2 \cdot \pi \cdot f_R)^2}{\left[\left[(2 \cdot \pi \cdot f_R)^2 - (2 \cdot \pi \cdot f_0)^2 \right]^2 + \frac{(2 \cdot \pi \cdot f_R)^4}{Q^2} \right]^{0.5}}$$

At the onset of fringe wrap, the motion of the scattering surface is shown in figure 1. Notice that there is a large amount of harmonic distortion, even though fringe wrap has not yet occurred. This will result in phase noise appearing at several harmonics of the fundamental motion frequency.

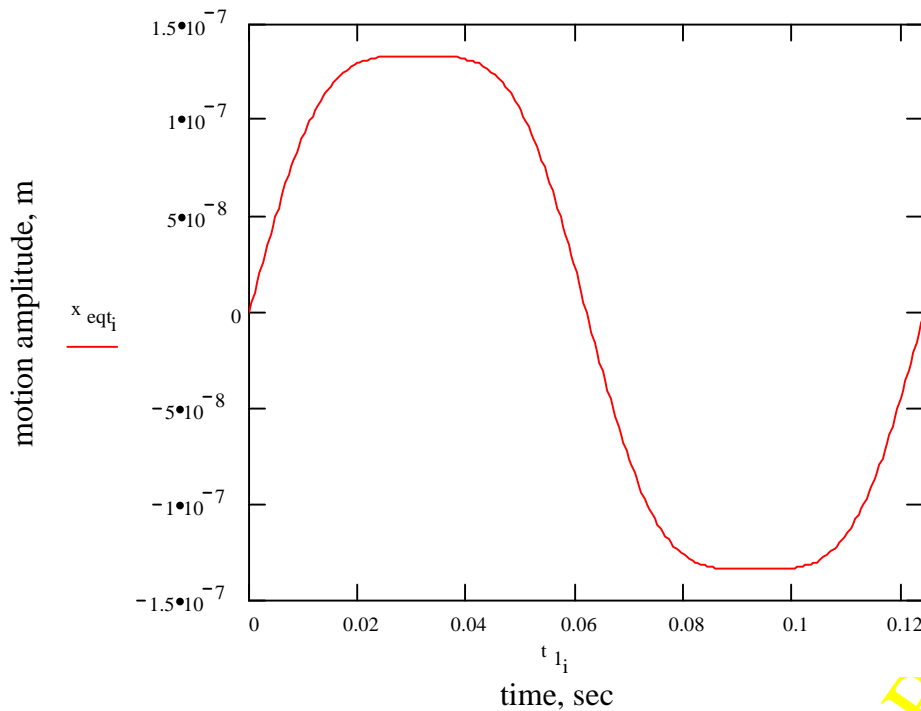


Figure 1: Displacement of scattering surface at the onset of fringe wrap

1. F. Raab and N. Solomonson, "Seismic Isolation Design Requirements Document" LIGO-T960065

2.1.2. Spectral Density of Scattering Surface Motion

The spectral density of the scattering surface motion is obtained by taking the Fourier transform of the time function $x_{eqf}(f)$. The maximum amplitude of the Fourier spectrum will be normalized by setting it equal to $\frac{\lambda}{8}$, since the effect of fringe wrapping is to clamp the surface amplitude at this value.

$$x_{eqfn}(f) = \frac{\lambda/8}{\max(x_{eqf}(f))} x_{eqf}(f).$$

2.1.2.1 Onset of Fringe Wrap

As an example, we will calculate the effective motion spectrum of a beam-dump with $Q=100$ moving with an amplitude of $\frac{\lambda}{8}$, which corresponds to the onset of fringe wrap. This will occur at a resonant frequency $f_0 = 8.05$ Hz. The spectrum of the effective scattering surface motion is plotted in figure 2, with reference to the standard LIGO ground spectrum and the resonant motion spectrum of the beam-dump. The effective motion within the LIGO gravitational wave band exhibits significant energy at the third and fifth harmonics of the fundamental frequency of the beam-dump vibration, e.g. 24.15 Hz and 40.25 Hz.

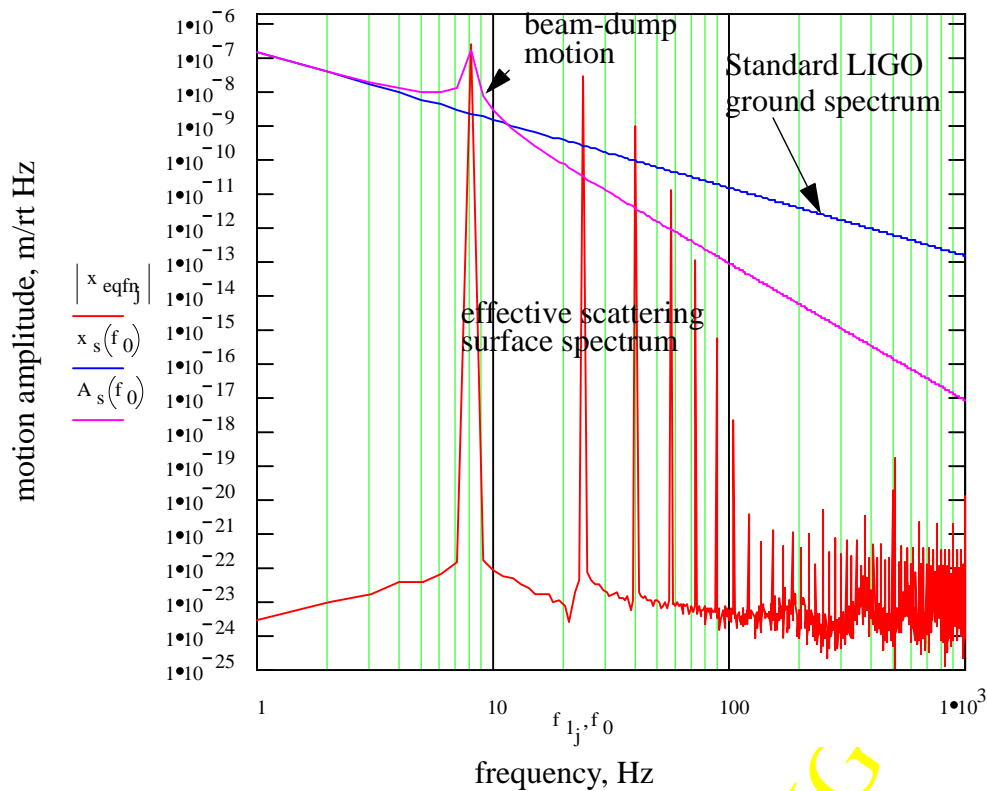


Figure 2: Amplitude spectrum of standard LIGO ground motion, resonant beam dump, and effective scattering surface motion at the onset of fringe wrap

2.1.2.2 Beyond Fringe Wrap

When the resonant amplitude of the beam-dump is increased by increasing the Q, e.g. $Q=200$; the beam-dump motion will exceed $\frac{\lambda}{8}$ at 8.05 Hz. The effective motion amplitude becomes clamped at $\frac{\lambda}{8}$, with fringe wrapping causing effective motions at higher harmonics, as shown in figure 3.

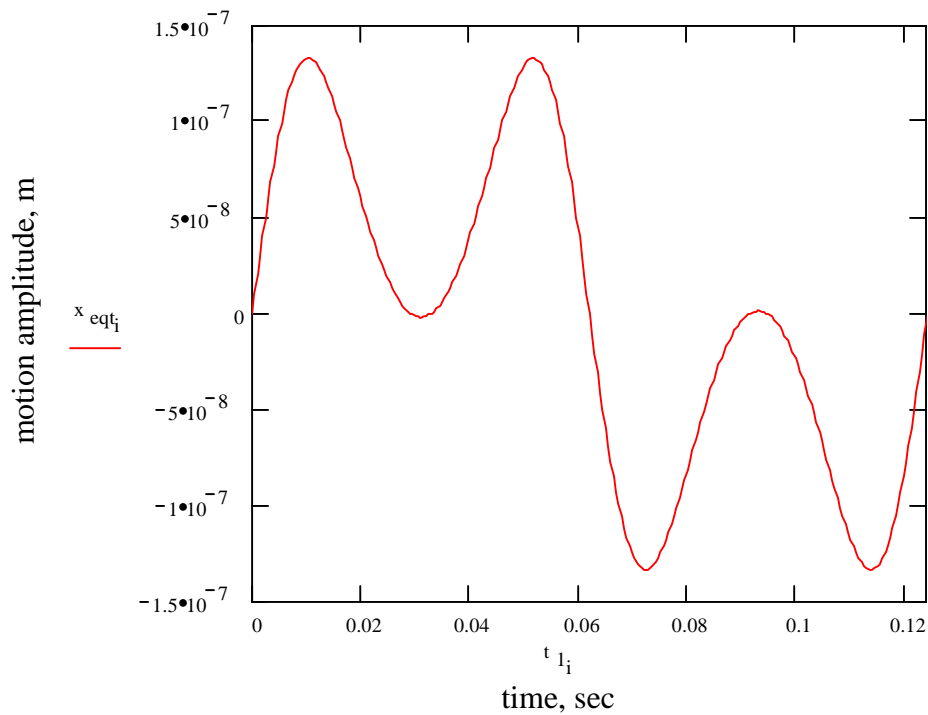


Figure 3: Displacement of scattering surface beyond fringe wrap

The amplitude of this motion significantly exceeds the LIGO ground motion amplitude within the gravity wave band at the higher harmonics of the fundamental frequency, as shown in figure 4.

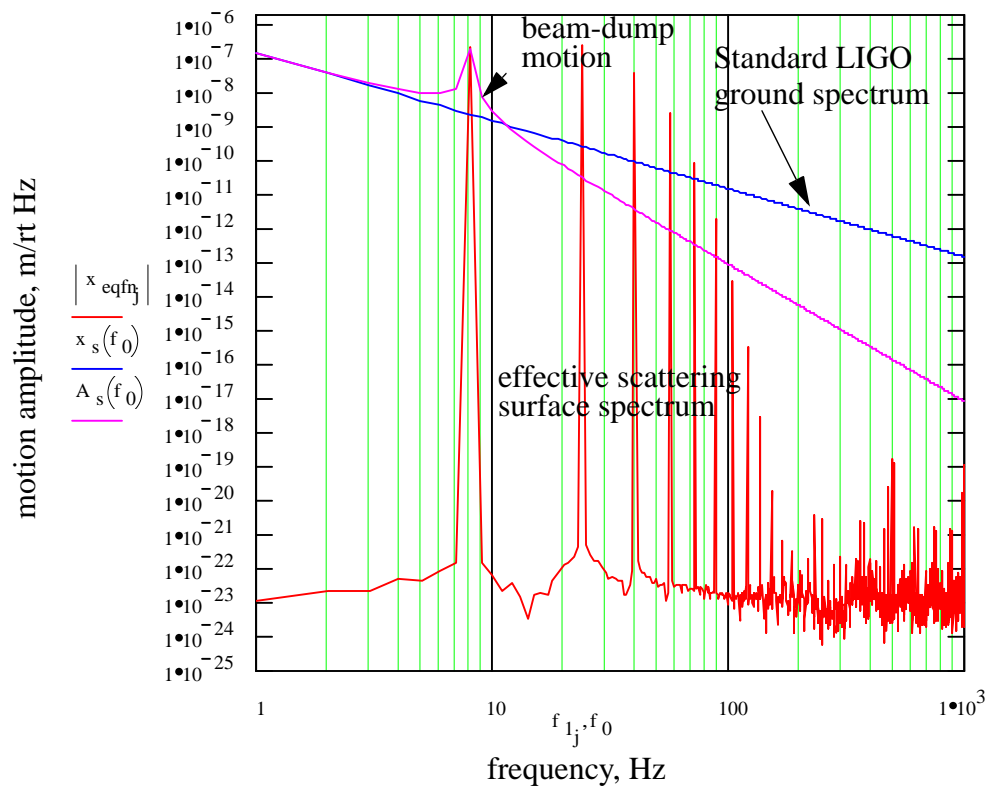


Figure 4: Amplitude spectrum of effective scattering surface beyond fringe wrap

2.1.2.3 Below Fringe Wrap

Provided the resonant frequency of the beam-dump is $>$ approximately 25 Hz, as shown in figure 5, the effective vibration amplitude of the beam-dump at the harmonics of the fundamental motion will not exceed the standard LIGO ground spectrum amplitude.

LIGO-DRAFT

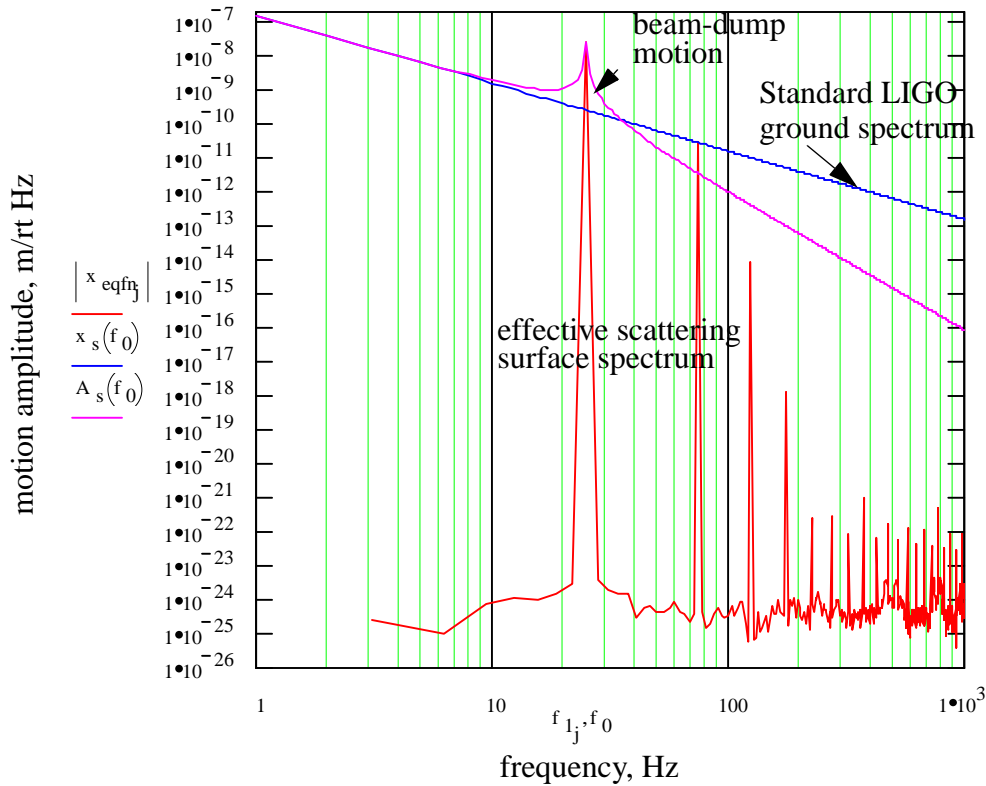


Figure 5: Amplitude spectrum of effective scattering surface motion with beam-dump resonance 25 Hz

3 EFFECT OF BEAM-DUMP MOTION AMPLITUDE ON SCATTERED LIGHT NOISE BUDGET

3.1. Noise Amplitude Ratio

The requirement for the maximum allowed scattered light into the LIGO IFO is that the phase noise field amplitude will not exceed 1/10 of the minimum gravity wave signal amplitude¹. The scattered light from the various scattering sources was budgeted to optimize the allocation of scattered light. Initially the majority of the budget was allocated to the PO beam paths, with the predominant scattered light noise sources being the PO beams photodetector surfaces. However, as the amplitude of the beam-dump motion increases due to the resonant amplification of the beam-dump structure, a larger portion of the budget allocation will be shifted to the ghost beam paths which scatter from the beam-dumps. At sufficiently large motions of the beam-dump surfaces, the scattered light from the beam-dumps will dominate the noise budget; especially the ghost beams ITMAR1.

1. COS Design Requirements Document, LIGO-T970071-02

The scattered light noise power due to scattering from the beam-dumps is dependent upon the Q of the beam-dump structure and the BRDF of the black glass absorbing surface. The total scattered light noise amplitude for all of the scattering sources is shown in figure 6, calculated for various values of damping $1/Q$ of the beam-dump structure with two values of scattering for the black glass surface, $BRDF = 1 \times 10^{-3} \text{ sr}^{-1}$, and $BRDF = 1 \times 10^{-4} \text{ sr}^{-1}$.

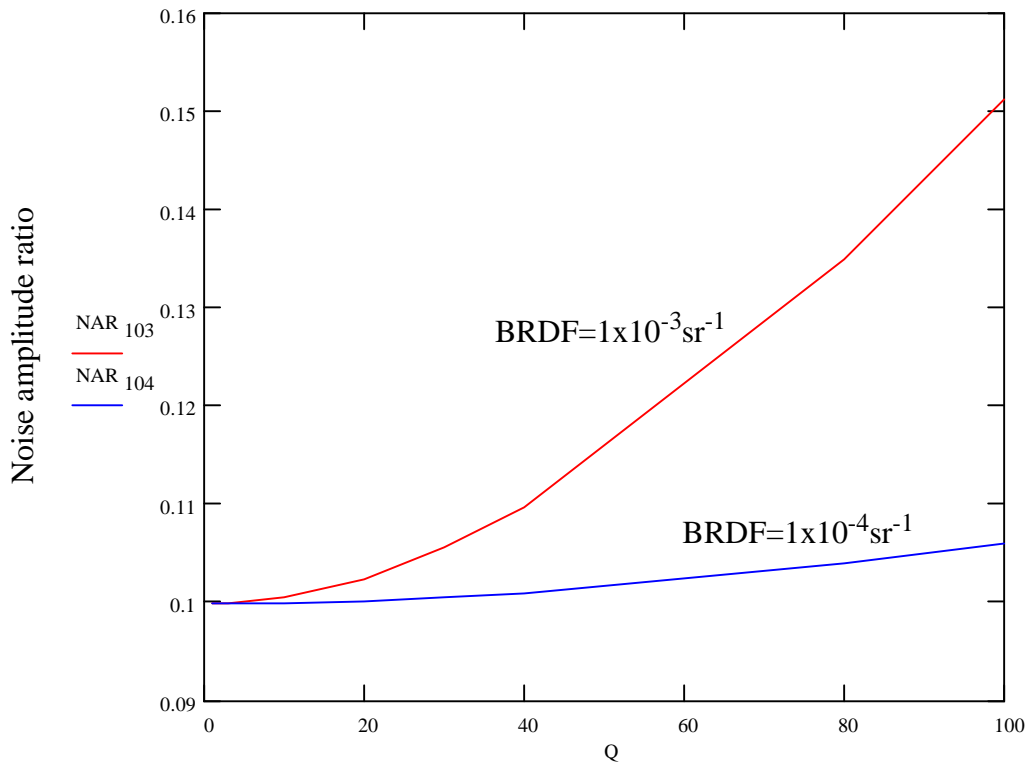


Figure 6: Scattered light noise amplitude ratio versus Q of beam-dump structure

From figure 6 we can see that with a $BRDF < 1 \times 10^{-4} \text{ sr}^{-1}$, scattered light from the surfaces of resonant beam-dump structures with $Q < 100$ contribute a negligible amount of phase noise for. With a worse scattering surface e.g. $BRDF = 1 \times 10^{-3} \text{ sr}^{-1}$, the Q must be < 40 to avoid a significant contribution from the beam-dump scattering.

3.2. Conclusion

3.2.1. BRDF of Black Glass

Preliminary measurements¹ of a sample of IR absorbing welder's glass indicated a value $BRDF = 1.4 \times 10^{-4} \text{ sr}^{-1}$ with p-polarization at an incidence angle of 55 deg.

3.2.2. Beam-dump Design

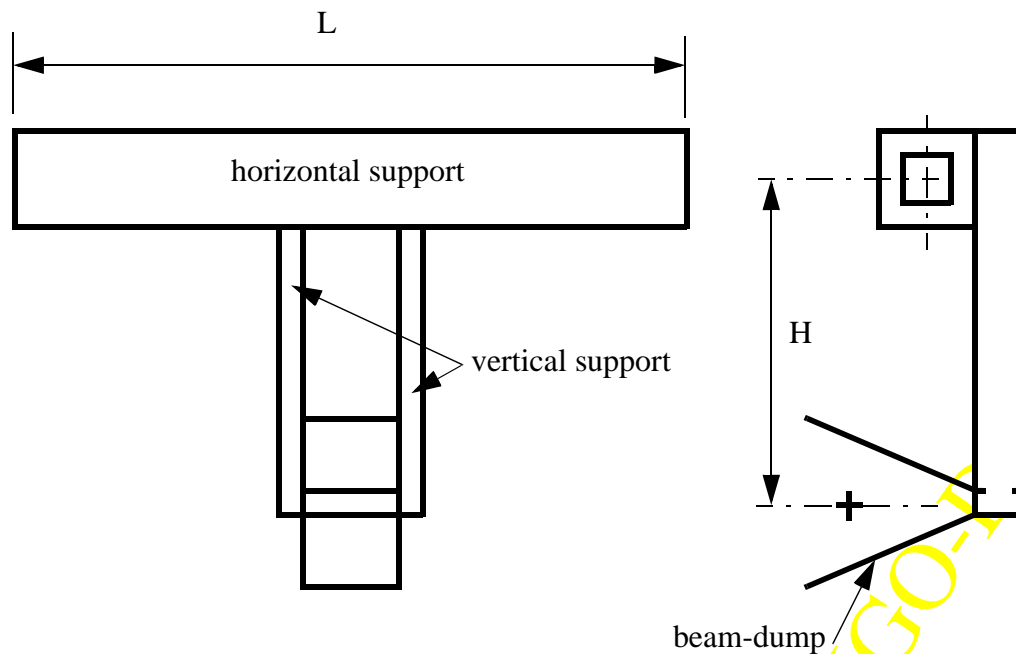
3.2.2.1 Triple Resonant Structure

The beam-dump structure will be modeled as a quadruple resonant structure, consisting of 1) the beam-dump, 2) the vertical support to hang the beam-dump, and 3) the horizontal beam to support the vertical support.

3.2.2.1.1 Horizontal Support

3.2.2.1.1.1 Torsional Resonance of Horizontal Beam

The horizontal beam has a fundamental torsional resonance due to the mass of the beam-dump and the distributed mass of the vertical support tubes offset with a lever arm from the axis of the horizontal beam, as shown schematically in the figure 7.



1. Rai Weiss, private communication 3/6/97

Figure 7: Schematic layout of beam-dump support structure

The effective spring constant for torsional bending of the horizontal support beam can be derived

$$k_{h\tau} = \frac{4JG}{H^2L},$$

where J is the polar moment of area of the beam cross-section, G is the shear modulus of elasticity, H is the lever arm to the location of the offset mass, and L is the length of the horizontal support tube.

The fundamental torsional resonant frequency of the horizontal support tube is given by

$$f_{RH} = \frac{1}{2\pi} \sqrt{\frac{k_{h\tau}}{m + m_v}},$$

where m is the mass of the beam-dump, and m_v is the effective distributed mass of the vertical support tubes located at the distance H; m_v is approximately equal to half the total distributed mass of the vertical support column.

3.2.2.1.1.2 Bending Resonance of Horizontal Beam

The effective spring constant for bending of the horizontal support beam can be derived

$$k_{hb} = \frac{[w_h L_h + (W_{vs} + 2W_{bd})]}{y_c},$$

where w_h is the weight per unit length of the horizontal beam, L_h is the length of the horizontal beam, W_{vs} is the weight of the vertical support tube, $2W_{bd}$ is the weight of two beam dumps, and y_c is the deflection at the center of the horizontal support beam.

The fundamental bending resonant frequency of the horizontal support beam is given by

$$f_{RH} = \frac{1}{2\pi} \sqrt{\frac{k_{hb}}{m_{hb}}},$$

where m_{hb} is the combined mass of the horizontal beam, vertical support column, and the two beam dumps.

3.2.2.1.2 Vertical Support

3.2.2.1.2.1 Bending Resonance of Vertical Tube

The vertical support has a fundamental bending resonance due to the mass of the beam-dump and the distributed mass of the vertical support beams, as shown schematically in the figure 7.

The effective spring constant for cantilever bending of the vertical support tube can be derived

$$k_v = \frac{3EI}{H^3},$$

where I is the moment of area of the tube cross-section, E is the modulus of elasticity, and H is the length of the vertical tube.

The fundamental bending resonant frequency of the vertical support structure is given by

$$f_{RH} = \frac{1}{2\pi} \sqrt{\frac{k_v}{m_v}},$$

where m_v is the combined mass of the vertical support tube and the two beam dumps.

3.2.2.1.2.2 Torsional Resonance of Vertical Tube

The effective torsional spring constant of the vertical support tube can be derived

$$k_{v\tau} = \frac{(J_v)(G_v)}{(r_{eff}^2)(h_1 + h_2)},$$

where J_v is the total polar moment of the vertical support tube, G_v is the shear modulus of the vertical tube, r_{eff} is the effective radius of the off-set beam dump weight, and $h_1 + h_2$ is the sum of the heights of the two beam dumps below the horizontal support tube.

The fundamental torsional resonant frequency of the vertical support structure is given by

$$f_{RH} = \frac{1}{2\pi} \sqrt{\frac{k_{v\tau}}{m_{bd}}},$$

where m_{bd} is the mass of the two beam dumps.

3.2.2.1.3 Beam-dump

The resonance of the beam-dump structure itself is too complicated for the simple model above. Consequently a WAG for the value will be made, which must be verified by a measurement.

3.2.2.2 Motion of the Beam-Dump Surface

The resonant frequencies of the double beam dump were calculated based on the following dimensions. All materials are aluminum.

| | |
|---|---------------|
| length of horizontal support beam, in | $L_h := 69$ |
| width of horiz. support beam crossection, in | $b_h := 4$ |
| height of horiz. support beam crossection, in | $h_h := 4$ |
| wall thickness of horiz. support beam, in | $t_h := 0.25$ |
| height of cross-section of vertical support, in | $h_v := 6$ |
| width of cross-section of vertical support, in | $b_v := 6$ |

LIGO-DRAFT

| | | |
|--|----------------------|---------------|
| wall thickness of vertical support, in | $t_v := 0.25$ | |
| length of vertical tube, in | $L_v := 22$ | |
| height to upper beam-dump, in | $h_1 := 6.469 - h_h$ | $h_1 = 2.469$ |
| height to lower beam-dump, in | $h_2 := 16.32 - h_h$ | $h_2 = 12.32$ |
| weight of beam-dump, # | $P_{bd} := 14$ | |

The displacement spectral density of the resonant beam dump structure driven by the standard LIGO seismic motion was calculated assuming the following Q values and the calculated resonant frequencies of the beam dump. The resonant frequency of the beam dump structure itself was assumed to be 200 Hz.

| | | |
|--|--|--------------------|
| Q of horizontal support beam | $Q_h := 50$ | |
| Q of vertical support beam | $Q_v := 50$ | |
| Q of beam-dump structure | $Q_{bd} := 50$ | |
| resonant frequency of horizontal support beam torsional, rad/s | $f_{h\tau} := 130$ | |
| resonant frequency of horizontal support beam bending, rad/s | $f_{hb} := 107$ | |
| bending resonant frequency of vertical support beam, rad/s | $f_{vb} := 681$ | |
| torsional resonant frequency of vertical support beam, rad/s | $f_{v\tau} := 365$ | |
| resonant frequency of beam-dump structure, rad/s | $f_{bd} := 200$ | |
| motion enhancement factor, horizontal bending | $A_{hb} := 1$ | |
| motion enhancement factor, horizontal torsion | $A_{h\tau} := 1$ | |
| motion enhancement factor, vertical bending | $A_{vb} := 1$ | |
| motion enhancement factor, vertical torsion | $A_{v\tau} := \tan\left(57 \cdot \frac{\pi}{180}\right)$ | $A_{v\tau} = 1.54$ |

The calculated beam dump surface motion spectral density is shown in figure 8.

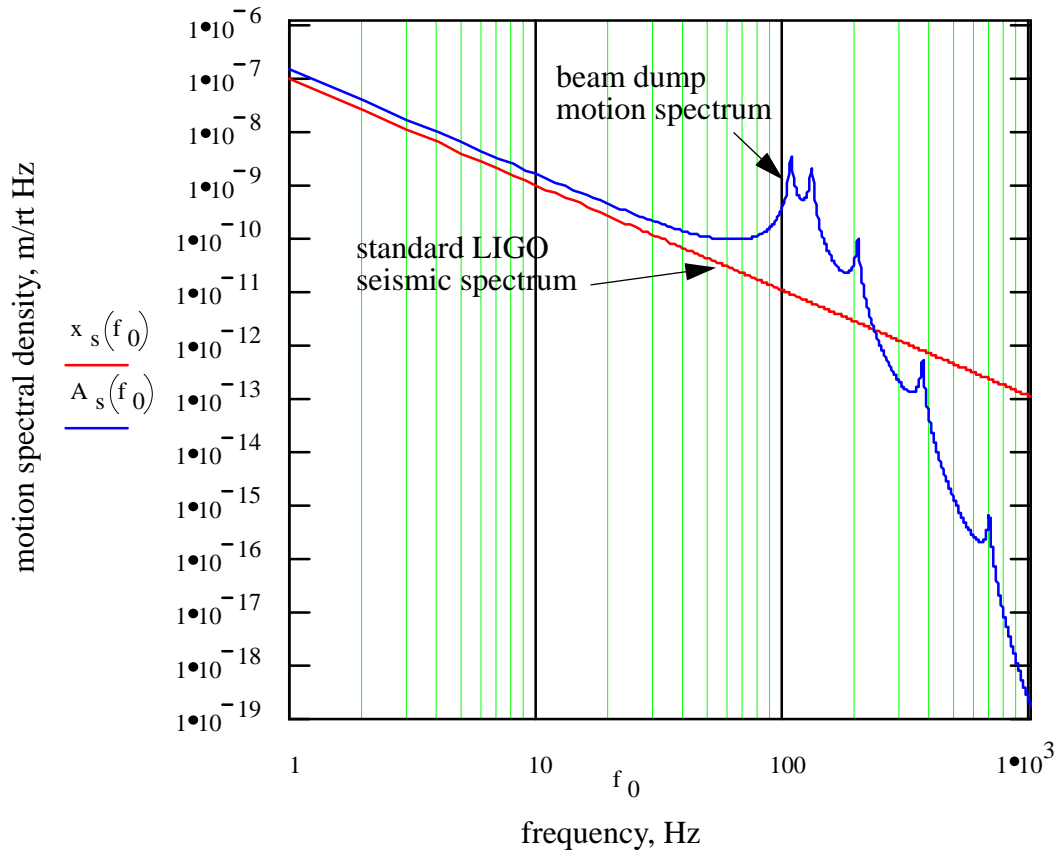


Figure 8: Surface motion spectral density of mounted beam dump assembly

Based on the analysis presented above, the beam-dump design will meet the scattered light requirements provided we use an absorbing surface with $BRDF < 1.4 \times 10^{-4} sr^{-1}$, a resonant frequency $> 25 Hz$, with a $Q < 100$.

LIGO-DRAFT